

Hiding and reading of information in a mechanochromic system of 2,5-dicarbazole-substituted terephthalate derivative

Pengchong Xue^a Zicheng Yang,^b Peng Chen,^b

^a Tianjin Key Laboratory of Structure and Performance for Functional Molecules, Key Laboratory of Inorganic-Organic Hybrid Functional Material Chemistry, Ministry of Education, College of Chemistry, Tianjin Normal University, No. 393, Bin Shui West Road, Tianjin, 300387, P.R. China.

^b Key Laboratory of Functional Inorganic Material Chemistry (MOE), School of Chemistry and Materials Science, Heilongjiang University, No. 74, Xuefu Road, Nangang District, Harbin, 150080, P. R. China

Corresponding author: xuepengchong@126.com

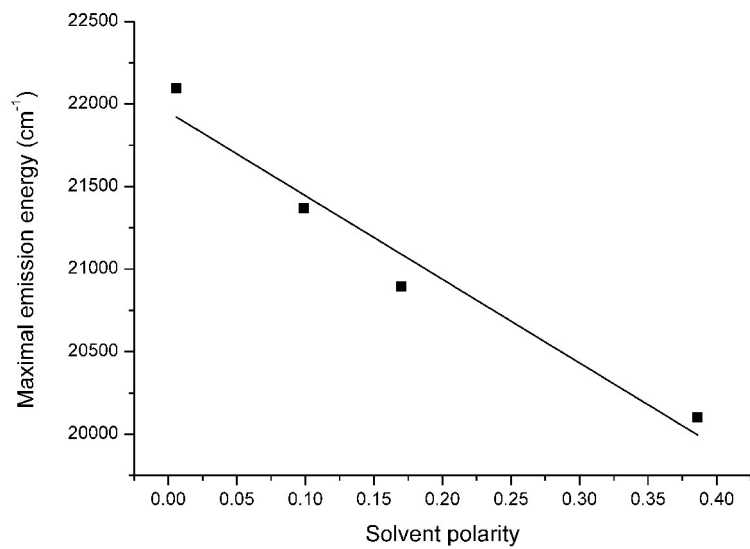


Fig. S1 Lippert–Mataga plot: fluorescence emission maximum energy of BOCTA as a function of solvent polarity.

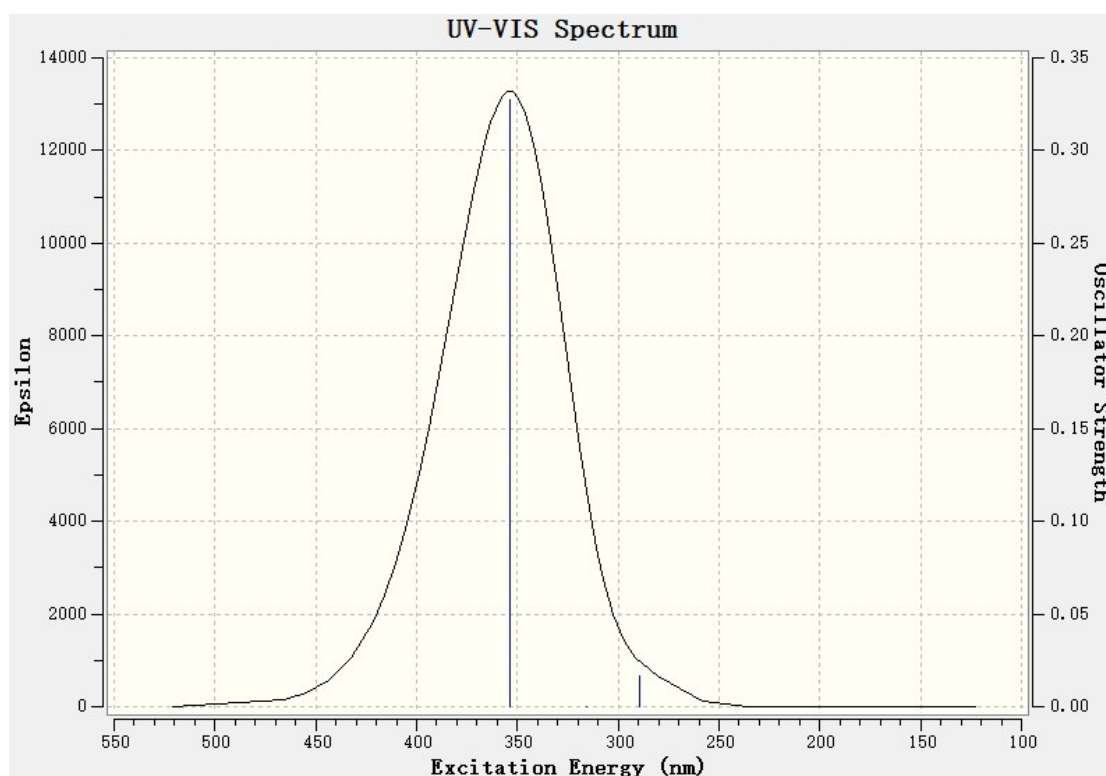


Fig. S2 Simulated absorption spectrum of BOCTA by the TD/DFT-CAM-B3LYP/6-31G(d) calculation.

Table S1. Photophysical data of BOCTA obtained by quantum chemical calculation.

	Transition assignment	E (eV)	λ_{abs} (nm)	Oscillator strength
	HOMO-4→LUMO (7.8%)			
BOCTA	HOMO-2→LUMO (4.6%)	3.5037 eV	353.87 nm	0.3277
	HOMO→LUMO (81.8%)			

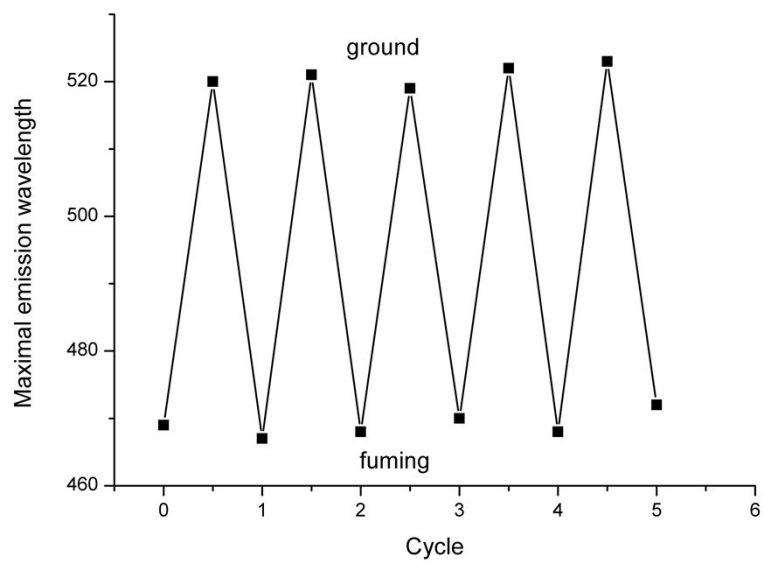


Fig. S3 Change of maximal emission wavelength during the grinding-fuming cycle.

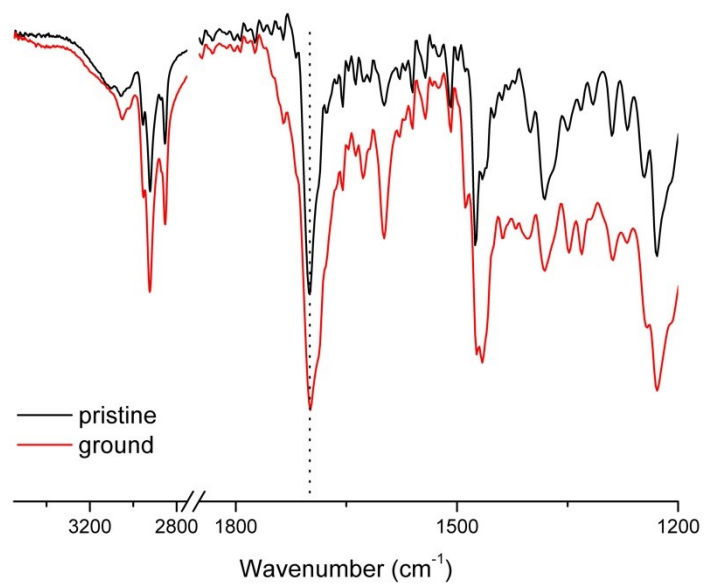


Fig. S4 FT-IR spectra of pristine and ground solids.

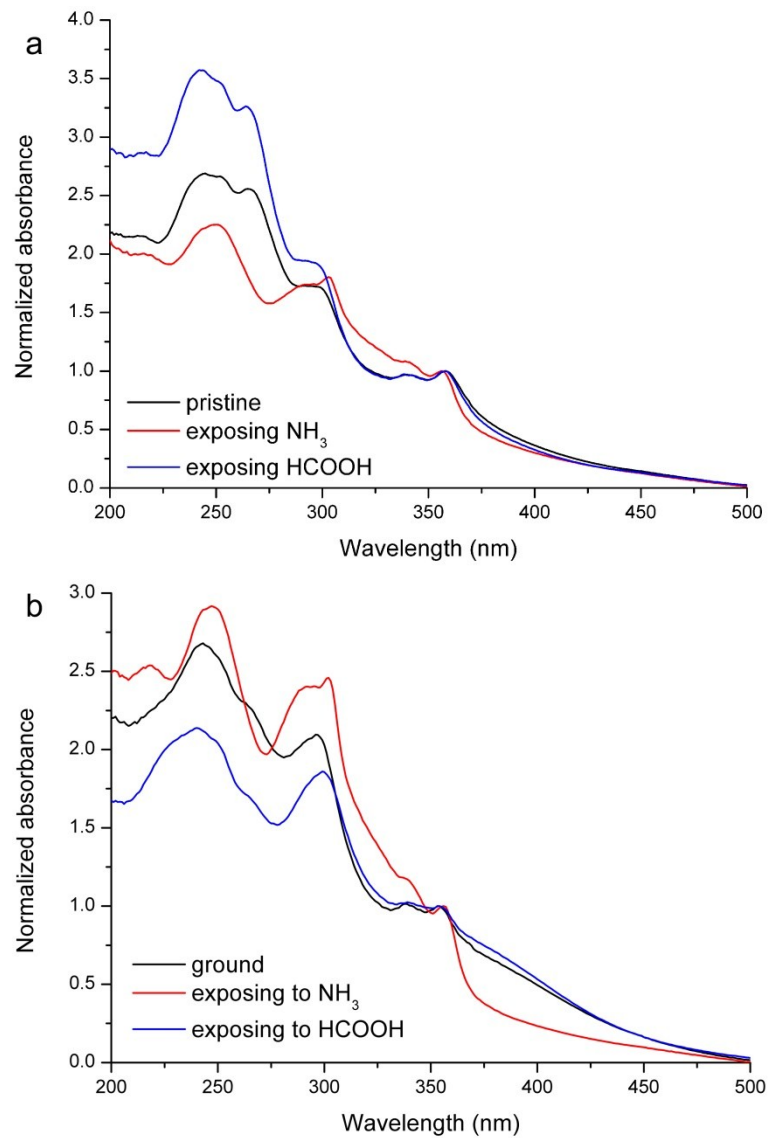


Fig. S5 UV-vis absorption spectra of (a) pristine and (b) solids upon exposure to NH_3 and then formic acid vapors.

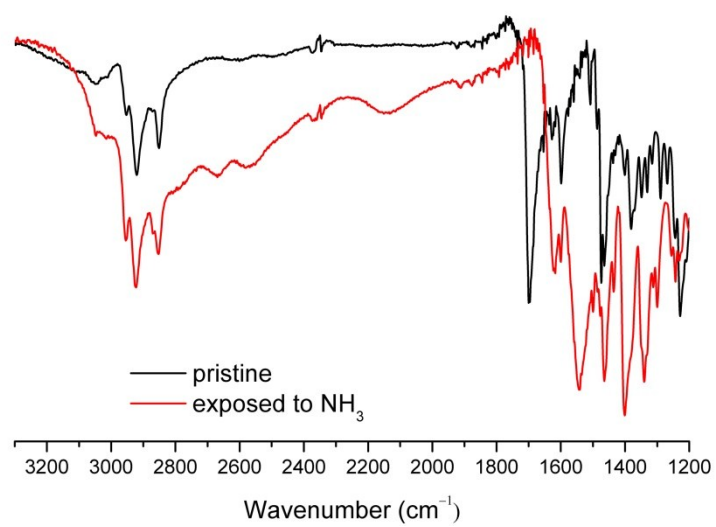


Fig. S6 FT-IR spectra of pristine and fumed solids.

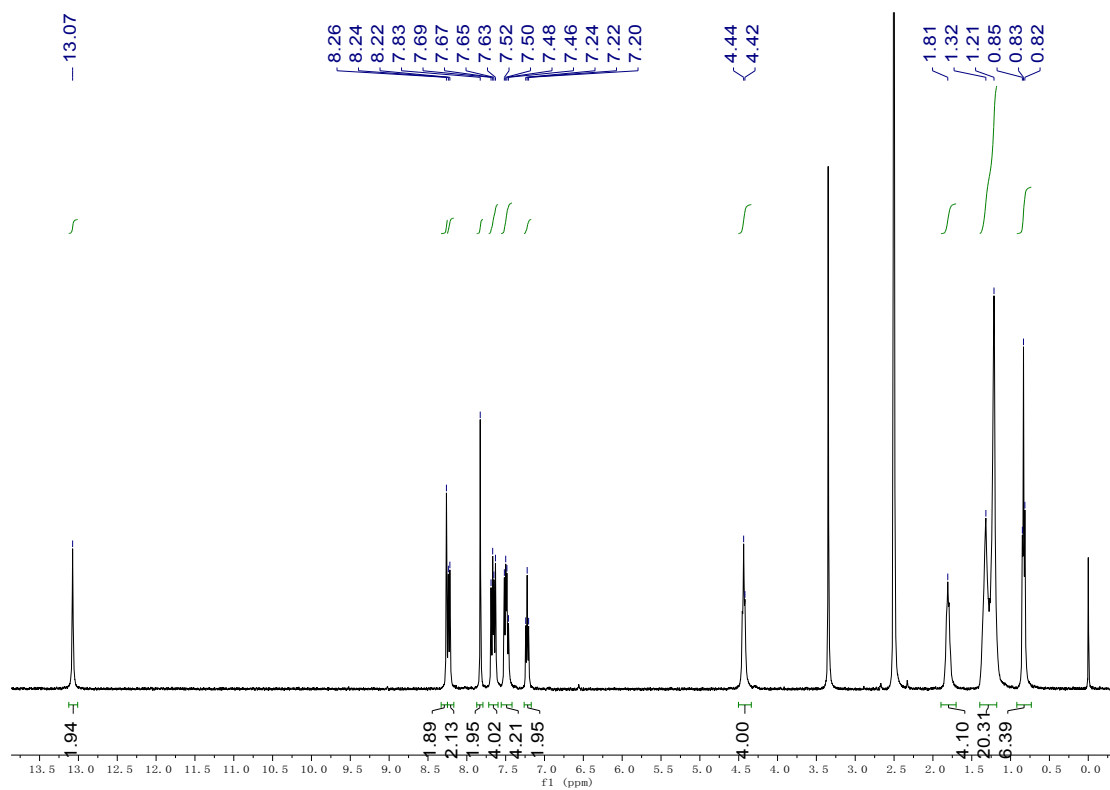


Fig. S7 ^1H NMR spectrum of BOCTA in D_6 -DMSO.

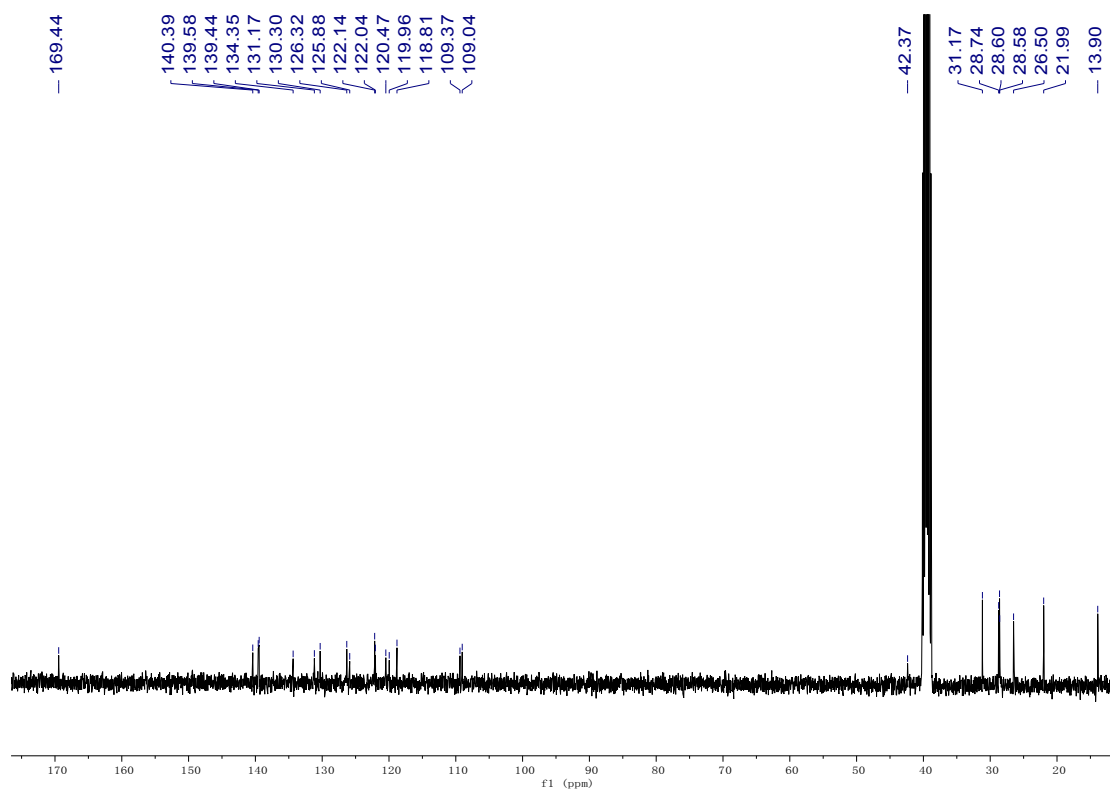


Fig. S8 ^{13}C NMR spectrum of BOCTA in D_6 -DMSO.

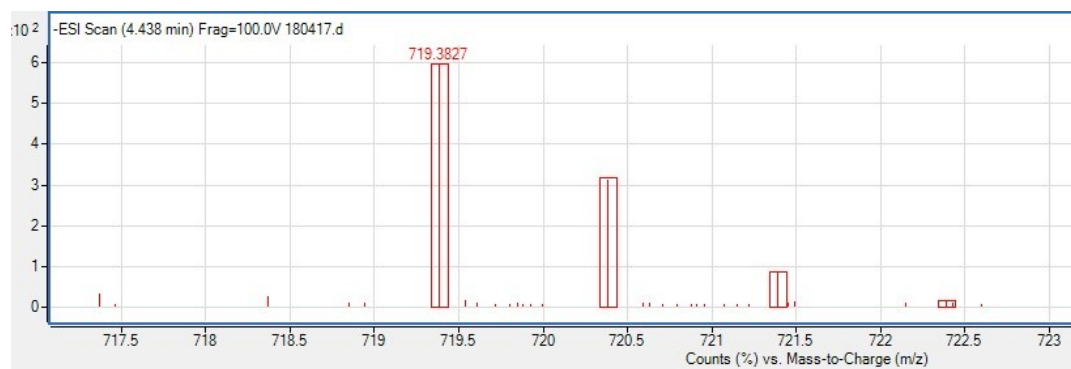


Fig. S9 HRMS spectrum of BOCTA as anion.